Polymer Entanglements

Richard P. Wool

Department of Materials Science and Engineering, University of Illinois, 1304 West Green Street, Urbana, Illinois 61801

Received June 8, 1992; Revised Manuscript Received December 31, 1992

ABSTRACT: Entanglements in concentrated random-coil flexible polymers are considered in terms of a network of bridges. A bridge is a segment of a polymer chain which is long enough to form one loop on itself. On the basis of a random-walk analysis, the onset of a bridge network is proposed to occur at the critical entanglement molecular weight $M_c = 30.89C_\infty M_0/\alpha^2 j$, where C_∞, M_0, and j are the characteristic ratio, monomer molecular weight, and number of backbone bonds per monomer, respectively. The factor α is determined by $\alpha = C/(bzj)$, where C, b, and z are the C-axis dimension of the unit cell, bond length, and number of monomers per C-axis length, respectively, and for many vinyl polymers $\alpha^2 j \approx 1$. The theoretical M_c expression, which contains no fitting parameters, was found to be in excellent agreement with experimental M_c values. The dependence of M_c on polymer concentration c, in the semidilute region was determined as $M_c \sim c^{-5/4}$, using the Blob model proposed by de Gennes and Daoud. The plateau modulus, $G_N°$, was found to depend on concentration as $G_N° \sim c^{9/4}$, which is in excellent agreement with experiment. The model predicts that the zero shear viscosity η_0 is affected by the entanglement connectivity and for reptating chains behaves as $\eta_0 \sim M^{3.4}c^{3.5}$.

Introduction

Entanglements develop from the interpenetration of random-coil chains and are important in determining rheological, dynamic, and fracture properties.[1] The subject has been reviewed by Graessley[2] and Aharoni[3] and more recently investigated by Kavassalis and Noolandi.[4] Of particular importance is the role of entanglements in controlling melt viscosity where the zero shear viscosity η_0, at low molecular weights M, behaves as a simple Rouse fluid with $\eta_0 \sim M$, and at high molecular weight $\eta_0 \sim M^{3.4}$. The crossover to a high-viscosity entangled fluid occurs at the critical entanglement molecular weight M_c. A similar effect is seen for the fracture energy G_{1C}, of glassy polymers such that when $M < M_c$, $G_{1C} \sim M$, and when $M > M_c$, $G_{1c} \sim M^x$, where x is of order 2–4, resulting in a sharp transition at M_c (reviewed in ref 5). Viscosity and fracture processes are both related to the transmission of forces through unit area (stress), and in this paper we examine the molecular structure capable of transmitting such forces in an entangled polymer melt.

Entanglement Model

An entangled amorphous linear chain network is shown schematically in Figure 1. The bridge model of connectivity in an amorphous network which we proposed[5,6] requires that the number of chain segments p crossing any load-bearing plane exceeds the number of chains n, by $p > 3n$. When $p < 3n$, a network cannot form and the chains readily slip apart by Rouse motion. When $p > 3n$, the chains are sufficiently interpenetrated to form an entanglement network and relaxation occurs by diffusion in the presence of entanglement constraints. At $p \approx 3n$, the polymer chains are critically connected and the average bridge structure has three crossings. This structure constitutes the unit "mesh" in the network.

The existence of an entanglement network in an isotropic concentrated melt can be explored by counting the number of bridges and chains intersecting an arbitrary plane, as shown in Figure 1. A bridge is a segment of chain which crosses the plane three times (bold section of chain in Figure 1). It is sufficiently long to complete one circular loop through the plane. The bridge is capable of transmitting forces across the plane in the melt for a time dependent on the relaxation of this chain segment. The number of chain segment crossings per unit area p is independent of molecular weight M in the virgin state, $p \sim M_0$. However, the number of chains n intersecting the plane decreases with increasing molecular weight as $n \sim M^{-1/2}$.[5,6] Thus, by varying the molecular weight, we can reach a state where the number of bridges is comparable to the number of chains.

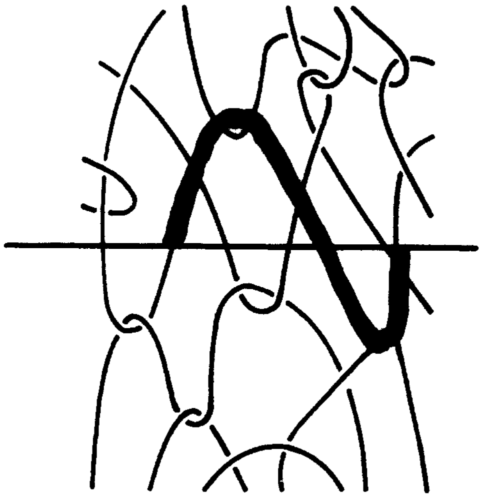

Figure 1. Entanglements in a polymer melt.

We define the number of bridges per chain p_c as

$$p_c = {}^1/_2(p/n - 1) \qquad (1)$$

such that when $p_c = 1$, $p/n = 3$, where the factor of 3 considers the three crossings per bridge. When $p_c < 1$, each chain contributes less than one bridge and the melt is not connected in a network. When $p_c > 1$, an entanglement network exists and we can determine M_c from the condition that $p_c = 1$, or $p = 3n$. This argument can be readily tested because, if the hypothesis is valid, M_c can be determined without any fitting parameters for all random-coil polymers, simply by calculating p and n, as follows.

The number of chains intersecting an arbitrary plane through random-coil chains is given in terms of the

0024-9297/93/2226-1564$04.00/0

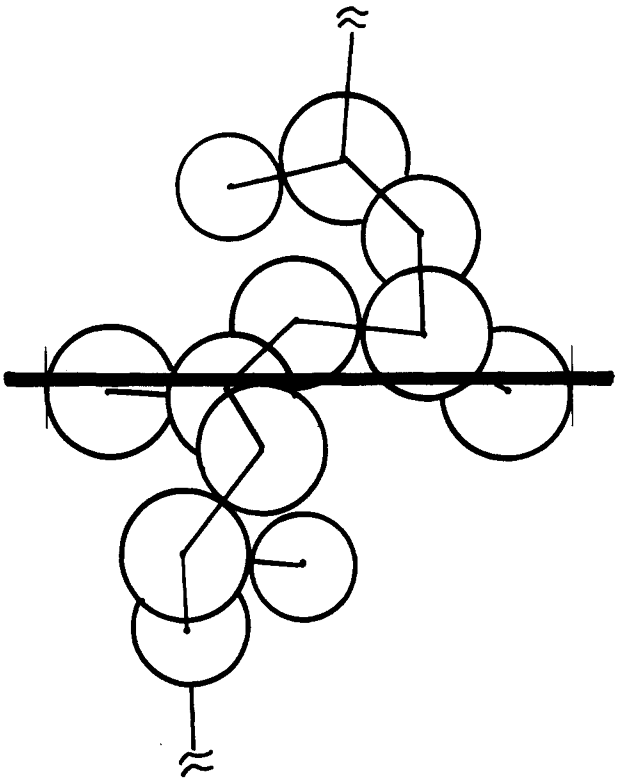

Figure 2. Chain segment with cross-sectional area.

molecular weight and random-coil parameters as[5,6]

$$n = 1.31[C_\infty j/(M_0 M)]^{1/2} b \rho N_a \quad (2)$$

where N_a, ρ, b, M_0, C_∞, and j are Avogadro's number, density, bond length, monomer molecular weight, characteristic ratio, and the number of bonds per monomer, respectively. Here $n = N_v\langle D\rangle$, in which the number of chains per unit volume $N_v = \rho N_a/M$ and $\langle D\rangle = 1.31N^{1/2}b$ is the diameter of a random-coil chain with N steps of length b.

The number of chain segment crossings per unit area in a concentrated melt is given by $p = 1/a$, where a is the projection of the cross-sectional area of the chain segment on the plane, as shown in Figure 2. When $p = 3n$ at M_c, then we obtain the critically connected network when the following condition is fulfilled:

$$3an = 1 \quad (3)$$

The cross-sectional area of the chain segment a could be determined from the monomer volume using $a = (M_0/\rho N_a)^{2/3}$. However, this approach tends to ignore the aspect ratio and details of chain structure due to conformation, such as helical segments and side groups. A more useful approach is to determine the molecular area from unit cell dimensions (when they exist) via the volume/length ratio, $a = 2^{1/2}V/L$, such that

$$a = 2^{1/2} z M_0/(C \rho N_a) \quad (4)$$

In this equation, the length L is the C-axis length (backbone direction) of the unit cell, the unit cell volume $V = zM_0/(\rho N_a)$, and z is the number of monomers per C-axis length. The factor of $2^{1/2}$ accounts for the random orientation of chains crossing the plane, compared with their perfect alignment in a crystal. During a mechanical deformation, the change in the orientation factor of the chains must be considered as the melt becomes anisotropic and the entanglement density changes with direction.[5]

Substituting for a, n, and p and solving for M_c at $p_c = 1$, we obtain the expression for the critical entanglement molecular weight as

$$M_c = 30.89(bz/C)^2 j M_0 C_\infty \quad (5)$$

in which all quantities are known, or can be estimated. Also, $(bz/C)^2 j \approx 1$, for many polymers, and an excellent approximation for M_c for vinyl ($j = 2$) polymers is obtained as

$$M_c \approx 30 C_\infty M_0 \quad (6)$$

Note that $M_c \sim C_\infty$, which means that stiffer chains have generally higher M_c values.

Kavassalis and Noolandi[4] devised a (KN) theory for N_e and N_c which is based on the number of other random-coil chains effectively constraining one particular chain in a tube as a function of molecular weight. They find that N_e is molecular weight dependent and reaches a lower asymptotic value with increasing molecular weight. N_c is related to N_e via $N_c = 27/4N_e$. If we identify N_e as the length of the chain to form one loop, then our model provides

$$N_c = 9/4N_e \quad (7)$$

Generally, one finds from experiment that $N_c \approx 2N_e$, with minor deviations. The KN theory determines M_c as

$$M_c \sim M_0^2/(\rho^2 C_\infty^3 b^6) \quad (8)$$

where the proportionality constant contains an unknown universal coordination number. The latter relation suggests that $M_c \sim C_\infty^{-3}$, which provides strong contrast with our result, viz., $M_c \sim C_\infty$. Aharoni[3] analyzed a large body of experimental M_c and structural data for flexible chains and found the empirical correlation $N_c \approx 10C_\infty^2$. There was enough scatter in the data to cast doubt on the exponent 2, but the general trend of N_c increasing with C_∞ was convincing. Our model predicts that $N_c \approx 60C_\infty$, when $(bz/C)^2 j \approx 1$ and $j = 2$. Also, from the definition of the characteristic ratio, $C_\infty = R^2/R_0^2$ and $N = R^2/b^2$, we expect $N_c = C_\infty N_0$ in which $N_0 = 30j$ at $C_\infty = 1$. To make an exact comparison with our model (eq 5), one needs to examine the relation $N_c = 30.89(bzj/C)^2 C_\infty$. A plot of N_c versus C_∞ as done by Aharoni and Wu[7] gives a proportionality factor $(bzj/C)^2$ which is different for each polymer and introduces natural scatter in their plot. Wu[7] also finds from analysis of M_e vs C_∞ data that $M_e \sim C_\infty^2$, in agreement with Aharoni. From the above arguments, we believe that this relationship is accidental.

Some exceptions to the M_c vs C_∞ trend are worth noting. For example, polymeric sulfur is very flexible with $C_\infty = 1.76$ but has a very large M_c value with $N_c \approx 3000$. Similarly, nitrocellulose and cellulose acetate with very large values of C_∞ have low values of M_c. Aharoni[3] makes an important distinction between flexible and rigid-rod polymers where the latter have relatively large characteristic ratios with $C_\infty \approx 50$. He notes that rigid-rod chains have very low N_c values compared to the more flexible chains with much lower C_∞ values. Thus, correlations of M_c with C_∞ are not independent of other physical factors such as high chain rigidity and polarity. Wu also finds that the yield stress and the stress σ_c to induce crazes in glassy polymers are both proportional to C_∞ and that $\sigma_c \sim M_c^{-1/2}$.

In our model, the number of steps N_c, to make one bridge, is determined from eq 5 as

$$N_c \approx 30 \quad (9)$$

This means that a random walker starting at a plane will need an average of about 30 steps to pass through the plane two more times. The latter problem is similar to

Table I
Molecular Properties

polymer	bond length b (Å)	C-axis length C (Å)	no. of monomers per C-axis z	monomer mol wt M_0	characteristic ratio C_∞	no. of backbone bonds per monomer j
polyethylene	1.54	2.55^c	1	28	6.7	2
polystyrene	1.54	6.5^a	3	104	10	2
polypropylene	1.54	6.5^a	3	42	5.8	2
poly(vinyl alcohol)	1.54	5.51^c	2	44	8.3	2
poly(vinyl acetate)	1.54	$6.5^{a,b}$	3	86	9.4	2
poly(vinyl chloride)	1.54	5.1^c	2	62.5	7.6	2
poly(methyl methacrylate)	1.54	10.4^d	4	100	8.2	2
poly(ethylene oxide)	1.51^e	19.48^f	7	44	4.2	3
polycarbonate	1.43^e	20.8	2	254	2.4	12

[a] 3/1 helix. [b] Assumed. [c] Planar zigzag. [d] Isotactic. [e] Average. [f] 7/2 helix.

the "Coin Toss" statistics problem where one bets a penny on "heads or tails" N times and keeps track of the number of times ones winnings or debt returns to zero, $Z(N)$. The number of crossings from winning to losing, $I(N)$, is equal to half the number of returns to zero plus 1, or

$$I(N) = 1 + Z(N)/2 \tag{10}$$

where

$$Z(N) = 1 + \sum_{r=0}^{\infty} W(N,r)/\sum W(N,r) \tag{11}$$

The function $W(N,r)$ is

$$W(N,r) = (N-r)!/[N!(N/2-r)!] \tag{12}$$

where r ranges from zero to infinity.

Equation 10 gives the number of crossings after $N = 30$ steps as $I(30) = 2.76$ which compares with our random-coil analysis with $I(30) = 3$. This value also compares with a random-walk computer simulation analysis with $I(30) = 2.74$ and with Bernoullian statistics which gives $I(30) = 3.19$. The value of $N_c \approx 30$ appears ubiquitous for entanglement segments with three crossings.

The relation for the molecular weight dependence of the number of bridges per chain is $p_c \sim M^{1/2}$. Since $p_c = 1$ at M_c, it follows that the proportionality constant is $M_c^{-1/2}$ such that

$$p_c = (M/M_c)^{1/2} \tag{13}$$

Thus, the total number of bridges per unit area in the virgin state is given by $p_\infty = p_c n$, as

$$p_\infty = 1.31[C_\infty j/(M_0 M_c)]^{1/2} b \rho N_a \tag{14}$$

The entanglement model presented above (eq 5), unlike all others, contains no adjustable parameters; it only contains known constants and, therefore, its utility can be tested by comparing the theoretical M_c with experimental M_c values. In the following sections, we examine the model's ability to predict M_c, its concentration dependence and rheological properties influenced by entanglements.

Applications of the Entanglement Model

Critical Entanglement Molecular Weight, M_c. In this section we compare experimental M_c values with those predicted by the entanglement model using

$$M_c = 30.89(bz/C)^2 j M_0 C_\infty \tag{15}$$

and where appropriate, using the short formula, $M_c \approx 30 M_0 C_\infty$. In the calculations below, the crystal data were obtained from Tadokoro's book[8] and M_c data from review tables in papers by Aharoni,[3] Wu,[7] Graessley,[2] and Ferry.[14]

Polyethylene. Using the parameters for polyethylene (PE) shown in Table I, the entanglement model gives $M_c \approx 4200$ which compares with experimental values $M_c \approx 4000$. A planar zigzag (all-trans) conformation of the PE chain in an orthorhombic unit cell was used to describe the cross-sectional area of the molecule. In the melt, we can expect many gauche conformers to be populated. However, the model is not very sensitive to the exact average conformational details because of compensating effects in the helix term α, given by

$$\alpha = C/(zjb) \tag{16}$$

Here, large excursions of the internal rotation angles only result in small changes in the length C, and when z increases, C also increases. However, changes in a are amplified by the α^2-contribution to M_c. The equation for M_c may be rewritten as

$$M_c = 30.89 C_\infty M_0/(\alpha^2 j) \tag{17}$$

The factor $\alpha^2 j$ is the difference between the exact and short formula for M_c. Note that $\alpha^2 j \approx 1$ for a 3/1 helix with $j = 2$. For a 2/1 all-trans PE helix, $\alpha = 0.827$, but for a 3/1 trans–gauche PE helix, $\alpha = 0.703$. The latter conformation would give $M_c \approx 5500$. The model predicts that we get an increase in M_c with increasing cross section of the chain, corresponding to a helix with a greater number of monomers per turn.

The short formula (eq 6) gives $M_c = 30 C_\infty M_0 = 5600$. Thus, for molecules related to the PE family, e.g., low-density polyethylene (LDPE), high-density polyethylene (HDPE), linear low-density polyethylene (LLDPE), and polymers containing large CH_2 sequences, such as polybutadiene, nylon 6, nylon 6-6, nylon 6-10, etc., we expect to have similar M_c values in the vicinity of $M_c \approx 4000$–5000, with some small variation due to differences in C_∞ and M_0. When the polymer molecule becomes highly polar or rigid, the model is not expected to work since new mechanisms of transmitting forces are introduced.

Polystyrene. For polystyrene (PS), we obtain $M_c \approx 32\,000$ from the data in Table I. The experimental value is given as $M_c = 31\,200$, although values as high as 36 000 and 38 000 have been reported.[14] The cross-sectional area of a PS molecule was determined from the isotactic approximation for the helix factor $\alpha = 0.703$. Syndiotactic and atactic configurations will have similar cross sections and also give good agreement with theory. To obtain $M_c = 36\,000$, the helix factor needs to change from $\alpha = 0.703$ to $\alpha = 0.654$, which represents a change from a 3/1 to about a 7/2 helix. The short formula gives $M_c = 31\,200$.

Derivatives of PS, such as poly(α–methylstyrene) (PAMS) should have similar M_c values. In the latter case, the reported value[2] is $M_c = 28\,000$ with $C_\infty = 10.5$ and $M_0 = 118$. Using eq 17, we calculate that $\alpha^2 j = 1.37$ and $\alpha = 0.828$ which suggests that PAMS forms a tighter helical structure than PS ($\alpha \approx 0.703$). If PAMS had the same α

value as PS, then we predict that $M_c \approx 39\,000$. When the methyl group is placed on the phenyl ring in the ortho-position, poly(*o*-methylstyrene) (POMS) forms a 4/1 helix with a periodicity of $C = 8.1$ Å such that $\alpha^2 j = 0.66$. Thus, if $C_\infty \approx 10$ for POMS, then we expect $M_c \approx 55\,000$ which is much higher than that of PS. The experimental value has not been reported for comparison.

Polypropylene. For polypropylene (PP), we obtain (from Table I) $M_c = 7600$ which compares with the experimental value $M_c \approx 7000$. Although the isotactic configuration can adopt many local conformations in the melt, the average helix factor of $\alpha = 0.7$ and $\alpha^2 j = 0.99$ is not expected to be changed. The short formula gives $M_c = 7300$.

Poly(vinyl alcohol). For poly(vinyl alcohol) (PVOH), we obtain (from Table I) $M_c = 7000$ which compares with experiment, $M_c = 7500$. Even though PVOH is atactic, it adopts a planar zigzag conformation in the crystalline state giving $\alpha = 0.89$ and $\alpha^2 j = 1.6$. Since the α value for a planar zigzag conformation cannot be increased further in the melt, then we would have to increase C_∞ from 8.3 to 8.89 to obtain better agreement with experiment. The short formula gives $M_c = 11\,000$ which is much higher than the experimental value due to the poor assumption in this case that $\alpha^2 j = 1$.

Poly(vinyl acetate). For poly(vinyl acetate) (PVAc), we predict (Table I) that $M_c = 25\,200$, which compares with $M_c = 24\,500$ from experiment. In this case, we did not have unit cell dimensions for this atactic amorphous polymer but could easily guess at the helix factor. Bulky side groups in vinyl polymers tend to produce 3/1 helices with $\alpha = 0.703$. The short formula gives $M_c = 24\,300$, which is in excellent agreement with experiment.

Poly(vinyl chloride). For poly(vinyl chloride) (PVC), we predict (Table I) that $M_c = 10\,700$ which compares with experiment, $M_c \approx 11\,000$, based on $M_c \approx 2M_e$. An orthorhombic unit cell was used with a planar zigzag conformation.[8] The short formula gives $M_c = 12\,600$ for PVC.

Poly(methyl methacrylate). For poly(methyl methacrylate) (PMMA), we predict (from Table I) that $M_c \approx 18\,000$, which compares to $M_c \approx 18\,400$ (using $M_c = 2M_e$). The C-axis length was determined from the isotactic conformation of the chain in an orthorhombic crystal. The short formula gives $M_c \approx 25\,300$ for PMMA, which is consistent with a 3/1 helix. The properties of PMMA are sensitive to the tacticity and conformation. For example, the characteristic ratio has values ranging from 7.4 for syndiotactic PMMA to 11.5 for some conventional PMMA. In the 3/1 helix approximation for the average cross section in the amorphous state, this variation in C_∞ gives M_c values ranging from 22 000 to 34 500. Graessley reports a value of $M_c = 31\,000$ for PMMA with $C_\infty = 8.7$. Wu cites a value of $M_e = 9200$ ($M_e \approx {}^1/_2 M_c$) with $C_\infty = 8.2$, and Aharoni cites $M_c = 31\,500$ with $C_\infty = 7.0$. These variations may be real since PMMA has many structural forms. The agreement between our model and experiment is not considered to be in jeopardy since we can account for this range of M_c values once the conformational details are known for a specific type of PMMA. Most commercially available PMMA is not pure and typically consists of a copolymer of methyl and ethyl acrylates. The latter monomer is used to provide thermal stability.

Poly(ethylene oxide). For poly(ethylene oxide) (PEO), we obtain $M_c = 5000$ (Table I) which compares with experiment, $M_c = 4400$. In Table I, the bond length $b = 1.51$ was determined from an average of two C–C and one C–O bonds. A 7/2 helix conformation was used in a monoclinic crystal to obtain the C-axis length. The short formula gives poor agreement with $M_c \approx 8800$ for PEO since $\alpha^2 j = 1.79$. If we use $\alpha \approx 0.64$ for a 7/2 helix (instead of $\alpha = 0.614$), we obtain $M_c = 4500$, which is closer to the experimental value. An analysis of poly(propylene oxide) gave similar agreement (Table II).

Table II
Theoretical and Experimental Critical Entanglement Molecular Weights, Mc

polymer	M_c experiment	M_c theory
polyethylene	4000	4200
polystyrene	31200	32000
polypropylene	7000	7600
poly(vinyl alcohol)	7500	7000
poly(vinyl acetate)	24500	25000
poly(vinyl chloride)	11000	10700
poly(methyl methacrylate)	18400	18000
poly(ethylene oxide)	4400	5000
poly(propylene oxide)	5800	5000
polycarbonate	4800	4300

Polycarbonate. For polycarbonate (PC; of Bisphenol A), we predict that $M_c = 4300$, which compares favorably with experiment, $M_c = 4800$. The agreement between theory and experiment in this case is gratifying considering the complexity of the PC molecule's structure. In Table I, the bond length $b = 1.43$ was obtained from the average of four C–O, six C=C, and two C–C bonds. The value of $j = 12$ was determined from the sum of (nonparallel) backbone bonds. The short formula should not be used for PC because $\alpha^2 j = 4.4$, and PC is not a simple vinyl polymer with $j = 2$ for which the formula was designed. Sundararajan proposed that $C_\infty \approx 1.8$ for PC, based on conformational energy maps of PC chains in which the contiguous phenyl groups interact synchronously.[9] If this theoretical C_∞ value is correct, then the model predicts that $M_c = 3200$, which is smaller than the experimental M_c value.

The predicted and experimental M_c values are summarized in Table II. We conclude that the entanglement model has ample ability to predict M_c values for random-coil polymers.

Concentration Dependence of M_c. A polymer with concentration c in solution can exist in dilute, semidilute, or concentrated states. In dilute solution, the polymer chains in the form of solvated random coils with radius of gyration $R_g \sim M^\upsilon$ do not overlap. The exponent υ depends on the quality of the solvent, being 1/3 for poor solvents, 1/2 for Θ solvents, and up to 3/5 for good solvents. With increasing concentration in the dilute region, the random coils overlap eventually at the critical concentration, $c^* \approx M/(N_a V)$, where $V = (4/3)\pi R_g^3$ is the volume occupied by the random-coil sphere. Thus we have the molecular weight dependence of the overlap concentration as $c \sim M^{(1-3\upsilon)}$.

When the concentration is in the range $c^* < c < 1$, the chains are in the semidilute entangled region. The static and dynamic properties of polymers in this region have been examined by de Gennes[1,10] and Daoud et al.[11] Their analysis of polymers in good solvents is represented by the blob model as shown in Figure 3. Here, a chain is divided into N blobs of average size ξ, known as the "screening length". Each blob is noninterpenetrating with the other blobs and behaves as a self-avoiding walk (SAW), solvent-swollen chain with exponent $\upsilon = {}^3/_5$.

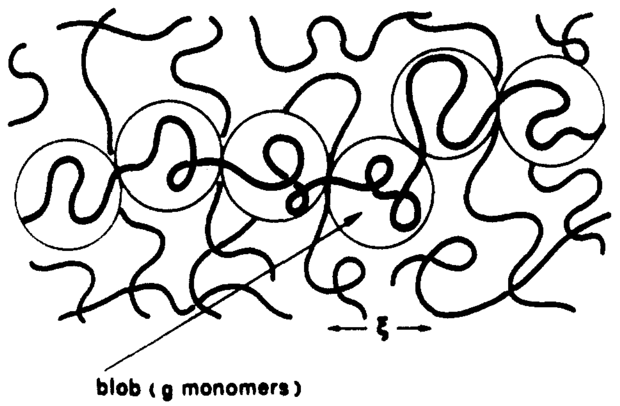

Figure 3. Blob model for a chain in the semidilute region.[1]

The concentration dependence of the screening length has been given as[1]

$$\xi(c) = R_g(c/c^*)^{\upsilon/(1-3\upsilon)} \tag{18}$$

With $\upsilon = {}^3/_5$, $c^* \sim M^{-4/5}$, and $R_g \sim M^{3/5}$, the latter equation gives the important result

$$\xi(c) \sim c^{-3/4} \tag{19}$$

Since each blob has the static properties of a SAW, the number of monomers in a blob, g, is related to ξ via $\xi \sim g^{3/5}$. From the latter two equations, it follows that $g \sim c^{-5/4}$. Since the number of blobs per chain is $N \sim M/g$, then the concentration dependence of N is obtained as

$$N(c) \sim c^{5/4} \tag{20}$$

This result will become the controlling factor for the concentration dependence of M_c and has been discussed by de Gennes,[10] Klein,[12] Wool,[5,6] and Kavassalis and Noolandi.[13] A critical experiment was conducted by Daoud et al.[11] using small-angle neutron scattering on deuterated polystyrene in a good solvent (carbon disulfide). They found that, in the semidilute region, $R_g^2/M \sim c^{-0.25}$ in agreement with $R_g^2 \sim N(c)\,\xi(c)^2$. This confirms their hypothesis that an entangled chain in the semidilute region obeys simple random-walk statistics while the blob has SAW characteristics.

We now examine our entanglement model to see if the blob model result $N(c) \sim c^{5/4}$ can be recovered from the conditions at critical connectivity (eq 3). When the number of bridges $p(c)/3$ equals the number of chains $n(c)$ intersecting any plane in the semidilute region, then we have from eq 1 that a critically connected state exists at $p_c = 1$ and

$$3n(c)\,a(c) = 1 \tag{21}$$

where $a(c)$ is the concentration-dependent cross section of a chain. Since $n(c) \sim N_v(c)\,R_g(c)$, where the number of chains per unit volume $N_v \sim c/M$ and $R_g(c) \sim M^{1/2}c^{-1/8}$, it follows that $n(c) \sim M^{-1/2}c^{7/8}$. *In terms of the dimensionless concentration* $\phi = c/\rho$, the concentration dependence of the number of chains per unit area obeys the scaling law

$$n(\phi) = n_\infty \phi^{7/8} \tag{22}$$

where $n_\infty \sim M^{-1/2}$ is determined at $\phi = 1$ using eq 2.

The chain segment cross section $a(c) = V/L$ is determined from the volume of the chain, $V = N\xi^3$, divided by its length, $L = N\xi$, such that $a(c) \sim \xi^2$. Therefore, $a(c) \sim c^{-3/2}$, or

$$a(\phi) = a(1)\,\phi^{-3/2} \tag{23}$$

where $a(1)$ is given by eq 4. Equation 23 requires that the blobs are close-packed and noninterpenetrating, which are basic assumptions of the blob model.

Substituting for $a(\phi)$ and $n(\phi) \sim M_c^{-1/2}$ in $3n(\phi)\,a(\phi) = 1$, we obtain the concentration dependence of M_c as

$$M_c(\phi) = 30.89(bz/C)^2 jM_0C_\infty/\phi^{5/4} \tag{24}$$

where $\phi^* < \phi < 1$, and all other parameters are determined at $\phi = 1$. This means that, when solvent is added to a polymer, its entanglement molecular weight increases (consistent with the blob model) and its entanglement density decreases as the chains swell. Equation 24 is in excellent agreement with experiments where it is found that $M_c(\phi) \sim \phi^{-x}$, in which the exponent $x \approx 1$, or slightly greater.[2,14]

Entanglement Density and Plateau Modulus. The entanglement density, υ_e, is determined by

$$\upsilon_e \sim \phi/M_c(\phi) \tag{25}$$

From eq 24, the entanglement density will have a concentration dependence in the semidilute region as

$$\upsilon_e(\phi) = \upsilon_e(1)\,\phi^{9/4} \tag{26}$$

where $\upsilon_e(1) = \rho N_a/M_e(1)$. This relation is important in solvent bonding and is related to the elastic properties of entanglement networks through the plateau modulus, $G_N°$, via the rubber elasticity relation

$$G_N° \sim \upsilon_e kT \tag{27}$$

where k and T are Boltzmann's constant and temperature, respectively. From eq 25, the concentration dependence of the plateau modulus is obtained at constant temperature as

$$G_N°(\phi) = G_N°(1)\,\phi^{9/4} \tag{28}$$

When solvent is added to an entangled polymer, ϕ decreases and the stiffness decreases approximately as ϕ^2. Graessley[2] examined the concentration dependence of $G_N°$ for PMMA and *cis*-polyisoprene and found that $G_N°$ was closely proportional to ϕ^2. Nagasawa and collaborators[15] examined polystyrenes with a range of molecular weights in solutions of benzyl *n*-butylphthalate at 100 °C and found that the exponent was between 2.2 and 2.3. Ferry[14] notes that $G_N°$ solution data for polybutadiene which does not require temperature reduction for comparison also gives an exponent between 2.2 and 2.3, in agreement with our model.

Viscosity and Relaxation Times. The zero shear viscosity $\eta_0(c)$, is determined as a function of concentration c by the Doi–Edwards theory[16] as

$$\eta_0(c) = G_N°(c)\,T_r(c) \tag{29}$$

where $T_r(c)$ is the concentration-dependent reptation time. $T_r(c)$ is given by

$$T_r(c) = \tau_0(c)\,[M/M_e(c)]^3 \tag{30}$$

in which $\tau_0(c)$ is the relaxation time of a single blob and $M_e(c)$ is the entanglement molecular weight corresponding to the onset of the plateau modulus. We assume that M_e and M_c have the same scaling properties and are related by $M_c \approx {}^9/_4M_e$. A single blob contains g monomers with a concentration dependence $g \sim c^{-5/4}$. The blob relaxation time $\tau_0(c)$ is determined by Rouse dynamics such that $\tau_0(c) \sim g^2$ and hence $\tau_0(c) \sim \tau_0(1)\,c^{-2.5}$. Substituting for $\tau_0(c)$ and $M_c(c) \sim c^{-5/4}$, the concentration dependence of the reptation time is obtained as

$$T_r(c) \sim T_r(1)\, c^{5/4} \qquad (31)$$

Substituting for $\tau_0(c)$, $G_N{}^\circ(c)$, and $M_c(c)$ in eq 29, we obtain

$$\eta_0(c) = G_N{}^\circ \tau_0(1)\,[M/M_e]^3 c^{3.5} \qquad (32)$$

The prediction that $\eta_0(c) \sim c^{3.5}$ is in excellent agreement with experimental data reviewed by Ferry.[14] However, the prediction that $\eta^0 \sim M^3$ contrasts with the generally accepted experimental law $\eta_0 \sim M^{3.4}$ and has been an unsolved problem for decades. Despite the closeness of exponents, 3.4 compared with 3.0, the exponent of 3.4 is unacceptable within the reptation framework for the following reason. The reptation time is related to the self-diffusion coefficient D and end-to-end vector R, by[1]

$$T_r = R^2/(3\pi^2 D) \qquad (33)$$

such that $D(c) = D(1)\, c^{-1.5}$. It is firmly established that $R^2 \sim M$, and this requires that $D \sim M^{-2.4}$ in order to have $T_r \sim M^{3.4}$. However, the exponent of −2.4 has not been realized in the majority of diffusion studies where the data strongly supports $D \sim M^{-2}$, which is consistent with $T_r \sim M^3$ in eq 33.

Our entanglement model suggests that the relaxation of the network occurs faster than the reptation time. Each stressed chain relaxes by reptation until a critically connected state is reached corresponding to $p_c = 1$. This is physically analogous to the vector percolation relaxation mechanism for networks discussed in refs 5 and 17. In order for a step strained network to relax to zero stress, it is not necessary for every bond to relax but only a certain fraction corresponding to the percolation threshold. The number of stressed bridges per unit area $p(t)$ is given by

$$p(t) = p_\infty[1 - (t/T_r)^{1/2}] \qquad (34)$$

where the term in brackets has the same time dependence as the stress relaxation modulus $G(t)$, in the Doi–Edwards function at $t < T_r$. The terminal relaxation time τ_c occurs at $p_c = 1$, corresponding to $p(t)/n_\infty = 1$, where the number of chains n_∞ remains constant. Since the entanglement model gives $p_\infty/n_\infty = (M/M_c)^{1/2}$, the terminal relaxation time is related to the reptation time $T_r \approx G_N{}^\circ\tau_0(M/M_e)^3$ by

$$\tau_c = G_N{}^\circ\tau_0(M/M_e)^3[1 - (M_c/M)^{1/2}]^2 \qquad (35)$$

When M becomes very large, the terminal time approaches T_r.

The fraction of the network which relaxes by reptation is $\Phi_r = [1 - (M_c/M)^{1/2}]$, and the fraction relaxing by Rouse-like processes is $\Phi_{RO} = (M_c/M)^{1/2}$. Letting $\eta_r = \Phi_r G_N{}^\circ\tau_c$ and $\eta_{RO} = \Phi_{RO} G_N{}^\circ\tau_{RO}$, where the Rouse time is related to T_r by $\tau_{RO} = 4/27(M_c/M)T_r$, we obtain the zero shear viscosity as

$$\eta_0 \sim G_N{}^\circ\tau_0(M/M_c)^3\{[1 - (M_c/M)^{1/2}]^3 + 4/27(M_c/M)^{3/2}\} \qquad (36)$$

The latter equation behaves empirically as $\eta^0 \sim M^{3.4}$ for $M > M_c$ and converges very slowly to an exponent of 3 with increasing molecular weight. Doi[18] derived a similar relation using a different physical concept, namely, chain-end fluctuation (CEF). In the CEF model, Doi proposes that Rouse-like fluctuations of the chain ends effectively shorten the tube length and result in a terminal relaxation time similar to that given in eq 35. Both models decouple the time dependence of the center-of-mass motion (diffusion) from stress relaxation (viscosity) and produce a pseudo 3.4 exponent. The concentration dependence of η_0 behaves as $\eta \sim c^{3.5}$ when $M \gg M_c(c)$, but eq 36 predicts that the apparent exponent will become very large in the vicinity of $M_c(c)$.

This entanglement model was also found to have useful applications to polymer interfaces where the strength is dominated by disentanglement mechanisms and in understanding the molecular weight dependence of fracture.[5]

Acknowledgment. The author is grateful to the Air Force Office of Scientific Research, Grant AFOSR-90-0242, via the Center for Cement Composite Materials at the Univeristy of Illinois, and to the Federation of Advanced Materials Industries (FAMI), for financial support of this research.

References and Notes

(1) de Gennes, P.-G. *Scaling Concepts in Polymer Physics*; Cornell University Press: Ithaca, NY, 1979.
(2) Graessley, W. W. *Adv. Polym. Sci.* **1982**, *16*, 1; **1982**, *47*, 67.
(3) Aharoni, S. M. *Macromolecules* **1983**, *16*, 1722.
(4) Kavassalis, T. A.; Noolandi, J. *Phys. Rev. Lett.* **1987**, *59*, 2674.
(5) Wool, R. P. *Structure and Strength of Polymer Interfaces*; Hanser Press: New York, 1993.
(6) Wool, R. P. *Rubber Chem. Technol.* **1984**, *57*, 307; *J. Elast. Plast.* **1985**, *17*, 107.
(7) Wu, S. *Polym. Eng. Sci.* **1990**, *30* (13), 753.
(8) Tadokoro, H. *Structure of Crystalline Polymers*; John Wiley and Sons: New York, 1979.
(9) Sundararajan, P. R. *Macromolecules* **1989**, *22*, 2149.
(10) de Gennes, P.-G. *Macromolecules* **1976**, *9*, 587; **1976**, *9*, 594.
(11) Daoud, M.; Cotton, J. P.; Farnoux, B.; Jannink, G.; Sarma, G.; Benoit, H.; Duplessix, R.; Picot, C.; de Gennes, P.-G. *Macromolecules* **1975**, *8*, 804.
(12) Klein, J. *Macromolecules* **1978**, *11*, 859.
(13) Kavassalis, T. A.; Noolandi, J. *Macromolecules* **1989**, *22*, 2709.
(14) Ferry, J. D. *Viscoelastic Properties of Polymers*; John Wiley and Sons: New York, 1980.
(15) Isono, Y.; Fujimoto, F.; Takeno, N.; Kajiura, H.; Nagasawa, M. *Macromolecules* **1978**, *11*, 888.
(16) Doi, M.; Edwards, S. F. *J. Chem. Soc., Faraday Trans.* **1978**, *2*, 74.
(17) Walczak, W. J.; Wool, R. P. *Macromolecules* **1991**, *24*, 4657.
(18) Doi, M. *J. Polym. Sci., Polym. Lett. Ed.* **1981**, *19*, 265.